AIP | Applied Physics Letters

Coexistence of conventional and inverse magnetocaloric effects and critical behaviors in Ni50Mn50−xSnx (x = 13 and 14) alloy ribbons

The-Long Phan, P. Zhang, N. H. Dan, N. H. Yen, P. T. Thanh et al.

Citation: Appl. Phys. Lett. **101**, 212403 (2012); doi: 10.1063/1.4767453
View online: http://dx.doi.org/10.1063/1.4767453
View Table of Contents: http://apl.aip.org/resource/1/APPLAB/v101/i21
Published by the American Institute of Physics.

Coexistence of conventional and inverse magnetocaloric effects and critical behaviors in $Ni_{50}Mn_{50-x}Sn_x$ ($x = 13$ and 14) alloy ribbons

The-Long Phan,[1] P. Zhang,[1] N. H. Dan,[2] N. H. Yen,[2] P. T. Thanh,[2] T. D. Thanh,[1,2] M. H. Phan,[3] and S. C. Yu[1,a)]
[1]*Department of Physics, Chungbuk National University, 361-763 Cheongju, South Korea*
[2]*Institute of Materials Science, Vietnam Academy of Science and Technology, Cau Giay, Hanoi, Vietnam*
[3]*Department of Physics, University of South Florida, Tampa, Florida 33620, USA*

(Received 19 September 2012; accepted 31 October 2012; published online 21 November 2012)

A systematic study of the conventional and inverse magnetocaloric effects and critical behaviors in $Ni_{50}Mn_{50-x}Sn_x$ ($x = 13$ and 14) alloy ribbons has been performed. We show that although the magnetic entropy change around the second-order ferromagnetic-paramagnetic (FM-PM) transition ($\Delta S_m \approx -4$ J/kg K) in the austenitic phase is about five times smaller than that around the first-order martensitic-austenitic (M-A) transformation ($\Delta S_m \approx 22$ J/kg K), the refrigerant capacity (RC) – an important figure of merit – is about two times larger for the former case (RC ≈ 160 J/kg) than for the latter case (RC ≈ 75 J/kg). This finding points to an important fact that to assess the usefulness of a magnetocaloric material, one should not only consider ΔS_m but also must evaluate both ΔS_m and RC. Our critical analysis near the second-order FM-PM transition reveals that Sn addition tends to drive the system, in the austenitic FM phase, from the short-range ($x = 13$) to long-range ($x = 14$) FM order. © *2012 American Institute of Physics*. [http://dx.doi.org/10.1063/1.4767453]

A temperature change (ΔT_{ad}) or a magnetic entropy change (ΔS_m) in a magnetic material subject to an external applied magnetic field under adiabatic conditions is known as the magnetocaloric effect (MCE).[1] This effect was first discovered in an iron sample and has long been explored in paramagnetic (PM) salts to attain temperatures below 1 K for cryogenic applications.[1,2] Recently, much attention has been paid to the discovery of magnetic materials exhibiting large MCEs around 300 K with potential for room-temperature magnetic refrigeration applications.[2–4] As compared to conventional vapour-cycle refrigeration techniques, magnetic refrigeration based on the MCE yields a higher cooling efficiency, leading to energy savings and limiting environmental pollution.[1] Before the potential of this technology can be fully realized, however, it is vital to develop materials that are cost-effective and exhibit large ΔS_m over a wide temperature range, namely a large refrigerant capacity (RC).[4] The RC is considered an important figure-of-merit for magnetic refrigeration and is determined not only by the magnitude of ΔS_m but also by its temperature dependence.[5–7] It has been reported that magnetic materials undergoing a field-induced/first-order magnetic phase transition (FOMT), such as $Gd_5(Si_xGe_{1-x})_4$, Mn-Fe-P-As, and $LaFe_{1-x}Si_xH_y$, show giant MCEs.[2,3] However, the observed MCEs are often restricted to narrow temperature ranges resulting in small values of RC. An opposite trend has been observed in materials displaying a second-order magnetic transition (SOMT).[5–7] In addition, hysteretic losses associated with the FOMT are usually very large and therefore detrimental to the RC, whereas these effects are very small or negligible in the case of the SOMT materials.[5]

$Ni_{50}Mn_{50-x}Z_x$-based Heusler alloys (Z = In, Sn, Sb, or Ga) are an interesting class of material as they have been reported to exhibit interesting physical phenomena, including exchange bias, FM shape memory, and giant MCEs.[8–12] It is worth mentioning that both conventional and inverse MCEs associated with negative and positive values, respectively, of ΔS_m coexist in these systems. While previous studies were mainly focused on exploring the inverse MCE in $Ni_{50}Mn_{50-x}Sn_x$ alloys and suggested that the large values of ΔS_m ($\sim$18–20 J/kg·K for $\mu_0\Delta H = 5$ T) observed in these alloys were ideal for active magnetic refrigeration.[8,10,11] Recent works have revealed that the hysteresis behavior is equally important and must be considered in evaluating the inverse MCE in these Heusler alloys.[13–15] In this context, it is essential to investigate the influences of FOMT and SOMT on the MCE and RC of the material. A systematic study of a correlation between the conventional MCE and critical parameters near the second-order FM-PM transition is also needed to shed light on the nature of magnetic interactions in the martensitic and austenitic phases in these systems.

In this letter, we attempt to address these important and unresolved issues by conducting a systematic study of the magnetocaloric effects and critical behaviors in melt-spun $Ni_{50}Mn_{50-x}Sn_x$ ($x = 13$ and 14) alloy ribbons, in which the austenitic phase coexists with ($x = 13$) or dominates over ($x = 14$) the martensitic phase. Our study highlights the fact that a large value of ΔS_m is not the sole factor in assessing the usefulness of a magnetocaloric material, as other figures of merit – in particular the RC – may be unfavorable. In addition, magnetic hysteresis losses must be taken into account in calculating the RC in the case of FOMT materials. Sn addition has also been shown to drive the $Ni_{50}Mn_{50-x}Sn_x$ system, in the austenitic ferromagnetic phase, from the short-range ($x = 13$) to long-range ($x = 14$) FM order.

$Ni_{50}Mn_{50-x}Sn_x$ alloy ribbons with $x = 13$ and 14 were fabricated by a melt-spinning method. Two initial ingots of $Ni_{50}Mn_{37}Sn_{13}$ and $Ni_{50}Mn_{36}Sn_{14}$ prepared by arc-melting from high-purity Ni, Mn, and Sn powders (4 N) were melted in a quartz crucible and ejected onto a spinning copper drum

a)Electronic mail: scyu@chungbuk.ac.kr.

with a tangential speed of 40 m/s. This process was carried out in an argon atmosphere. The resultant ribbons had a width and thickness of approximately 2 mm and 30 μm, respectively. Before the preparation of the ingots, investigations on the compensation of the elements with a low-melting point (such as Sn and Mn) were carried out carefully to achieve alloys with the expected compositions. Room-temperature structural analyses of the obtained ribbon samples using x-ray diffraction (XRD) revealed that besides the main phase corresponding to an austenitic $L2_1$-cubic structure (space group: $Fm3m$) with a lattice parameter of $a = 5.983$ Å for $x = 13$ and $a = 5.992$ Å for $x = 14$, there is a trace amount of an additional phase, which is assigned to an orthorhombic structure of 10M martensite (space group: $Pmma$). The intensity of XRD peaks related to this secondary phase decreases quickly with increasing Sn content in $Ni_{50}Mn_{50-x}Sn_x$, due to the development of the austenitic phase.[7] The magnetic and magnetocaloric properties of the samples were measured by using a superconducting quantum interference device (SQUID), where the temperature and applied magnetic field varied from 4.2 to 360 K and from 0 to 5 T, respectively. The temperature interval between magnetic field isotherms was 2 K near the phase transition temperatures and 5 K in other regions. Magnetic measurements were carried out using a warming protocol.

Figure 1 shows the temperature dependence of zero-field-cooled (ZFC) and field-cooled (FC) magnetizations, $M_{ZFC}(T)$ and $M_{FC}(T)$, for $Ni_{50}Mn_{50-x}Sn_x$. Under an applied field (H) of 15 mT, Figs. 1(a) and 1(b) show the feature of samples with structural and magnetic phase transitions.[1,9,16] With increasing temperature, the $x = 13$ sample exhibits a phase transition at ~250 K, which is known as the Curie temperature of the martensitic phase (T_C^M).[1] This transition is absent in the $x = 14$ sample, because the crystalline fraction of the austenitic phase is dominant. A first-order M-A transition occurs in both samples, with $T_{M\text{-}A} = 255$ K for $x = 13$ and 165 K for $x = 14$. The downward shift of $T_{M\text{-}A}$ for $x = 14$ is consistent with previous observations that Sn-doping contributes to the development of the austenitic phase, eventually leading to the complete suppression of the M-A transition for $x > 18$.[9,16] A separation between $M_{FC}(T)$ and $M_{ZFC}(T)$ appears at the so-called irreversibility temperature of 235 K ($<T_C^M$) for $x = 13$ and 178 K ($< T_{M\text{-}A}$) for $x = 14$. The degree of this separation has been seen to grow larger in alloys with lower Sn content, where the martensitic phase was dominant and different types of structure (such as 10M, 14M, and $L1_0$) coexisted.[9] In other words, the coexistence of FM and AFM interactions, and/or FM clusters in $Ni_{50}Mn_{50-x}Sn_x$ alloys could create short-range FM ordering states in the martensitic phase that is manifested in the FC-ZFC splitting of the magnetization.[9,16] For $T > T_{M\text{-}A}$, a FM-PM transition (T_C^A) appears in the austenitic phase. The values of T_C^A determined from the minima of dM/dT curves are 302 K for $x = 13$ and 310 K for $x = 14$. Notably, a hump indicated by asterisks in Figs. 1(a) and 1(b) can be related to inhomogeniety in crystal structure or to the presence of FM clusters, which often appear around the martensitic-start temperature.[9] This feature has been only observed in $Ni_{50}Mn_{50-x}Sn_x$ ribbons subject to low applied fields but disappeared as the applied field became sufficiently high (see Fig. 1(c), $M_{FC}(T)$ curves for $\mu_0 H = 1.2$ T).

To evaluate the MCE in the $Ni_{50}Mn_{50-x}Sn_x$ ($x = 13$ and 14) samples, isothermal magnetization, $M(H)$, curves were measured around the phase transition temperatures for different magnetic fields up to 5 T. Figure 2 shows $M(H)$ curves recorded at selected temperatures. For $x = 13$, at temperatures below 245 K, the 5 T magnetization decreased gradually with increasing temperature (Fig. 2(a)), due to the FM-PM transition in the martensitic phase. At higher temperatures from 245 to 258 K, however, besides a sharp increase in the magnetization, a sudden change of slope can be observed in the $M(H)$ curves at ~3.8 T, which is associated with the metamagnetic M-A transition.[8,9,16] Above 258 K, the metamagnetic behavior disappears and high-field magnetization decreases with increasing temperature as T_C^A is approached. The $x = 14$ sample (Fig. 2(b)) exhibits a similar temperature dependence of the $M(H)$ curves, with the appearance of the metamagnetic feature occurring at ~4.5 T in the temperature range of 150–170 K. We note that the values of saturation magnetization (M_s) in the ferromagnetic austenitic phase are significantly larger for $x = 14$ ($M_s \approx 80$ emu/g) than for $x = 13$ ($M_s \approx 55$ emu/g).

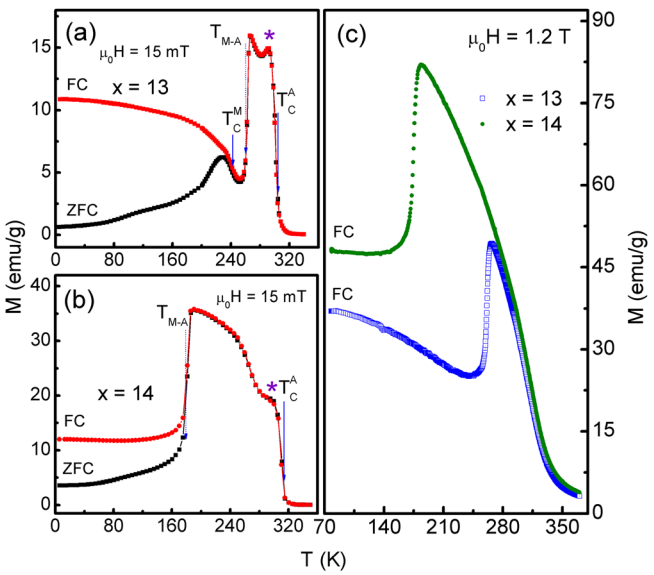

FIG. 1. $M_{ZFC}(T)$ and $M_{FC}(T)$ for $Ni_{50}Mn_{50-x}Sn_x$ alloy ribbons under applied fields of (a), (b) 15 mT, and (c) 1.2 T.

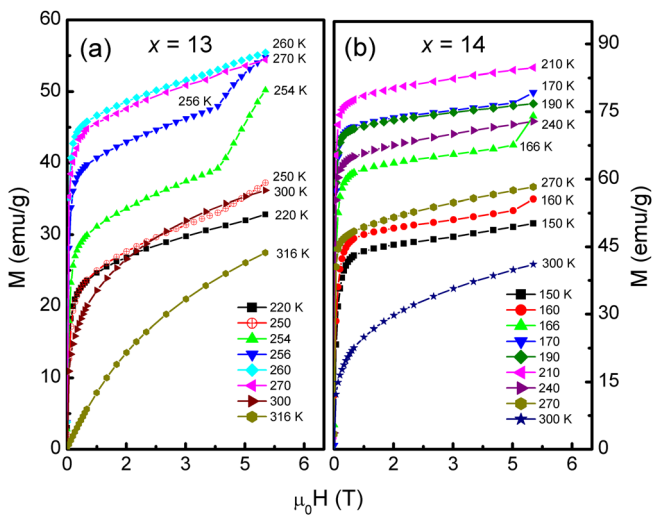

FIG. 2. Representative $M(H)$ curves for (a) $x = 13$ and (b) $x = 14$ alloy ribbons recorded at different temperatures.

From the $M(H)$ isotherms shown in Fig. 2, the ΔS_m of the $Ni_{50}Mn_{50-x}Sn_x$ ($x = 13$ and 14) samples has been calculated using the Maxwell relation[1]

$$\Delta S_m = \mu_0 \int_0^H \left(\frac{\partial M}{\partial T}\right)_H dH, \quad (1)$$

where M is the magnetization, H is the magnetic field, and T is the temperature.

Figure 3 shows temperature dependence of ΔS_m of the samples for applied fields up to 5 T. It can be observed that both conventional (negative) and inverse (positive) MCEs coexist, with an increase of the applied field enhancing absolute values of ΔS_m. For $\mu_0 \Delta H = 5$ T, the maximum magnetic entropy change, ΔS_{max}, associated with the inverse MCE are 22 J/kg K and 20 J/kg K around $T_{M\text{-}A} = 255$ K and 165 K for $x = 13$ and 14, respectively. These values are greater than those of a $Ni_{50}Mn_{37}Sn_{13}$ ingot ($\Delta S_{max} \approx 18$ J/kg K)[1] or $Gd_5Si_2Ge_2$ ($|\Delta S_{max}| \approx 19$ J/kg K).[2] However, the large ΔS_{max} values are only retained in a very narrow temperature range ($\Delta T_{FWHM} \approx 5$ K) due to the nature of the first-order M-A phase transformation. The resultant RC values are therefore expected to be relatively small, as shown below.

For the case of conventional MCE with negative ΔS_m values, the minima of the $\Delta S_m(T)$ curves occurred at T_C^A for both samples. For $\mu_0 \Delta H = 5$ T, the values of $|\Delta S_{max}| \approx 4$ J/kg · K in the austenitic range are relatively small, but the $\Delta S_m(T)$ curves are distributed over a wide temperature range ($\Delta T_{FWHM} \approx 58$ K and 97 K for $x = 13$ and 14, respectively), due to the nature of the SOMT. The broadening of $\Delta S_m(T)$ curves around T_C^A can be expected to enhance RC of the samples. In addition to the absolute minima associated with T_C^A, the $x = 13$ sample also exhibited an additional minimum with $|\Delta S_{max}| \approx 1$ J/kg · K for $\mu_0 \Delta H = 5$ T around 225 K, which can be attributed to the Curie temperature of the martensitic phase.

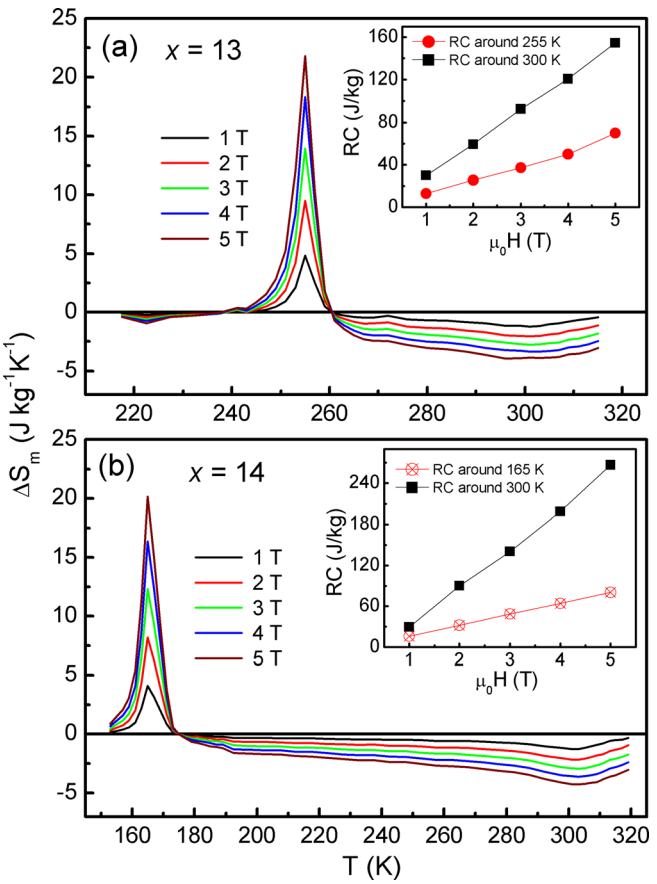

FIG. 3. $\Delta S_m(T)$ curves for $Ni_{50}Mn_{50-x}Sn_x$ ribbons with (a) $x = 13$ and (b) $x = 14$ under applied fields of 1–5 T. The insets of each figure correspond to magnetic-field dependences of RC around the phase-transition temperatures of $T_{M\text{-}A}$ and T_C^A.

As noted above, the RC is an important factor in assessing the usefulness of a magnetocaloric material. The RC values of the $Ni_{50}Mn_{50-x}Sn_x$ ($x = 13$ and 14) samples have been calculated from the relation[17]

$$RC = -\int_{T_1}^{T_2} \Delta S_m(T) dT, \quad (2)$$

where T_1 and T_2 are the temperatures of the cold end and the hot end of an ideal thermodynamic cycle, respectively, defined by the full width at half maximum of the $\Delta S_m(T)$ peak. The RC is plotted as a function of magnetic field and the results are displayed in insets of Fig. 3 for the cases around $T_{M\text{-}A}$ and T_C^A. As one can see clearly in these insets, the RC increased in alloys with higher Sn contents. It is worth noting that for $\mu_0 \Delta H = 5$ T, the ΔS_m around T_C^A ($\Delta S_m \approx -4$ J/kg K) is about five times, in magnitude, smaller than that around $T_{M\text{-}A}$ ($\Delta S_m \approx 22$ J/kg K), but the RC is about two times larger for the former case (RC ≈ 160 J/kg) than for the latter case (RC $\sim$75 J/kg). Furthermore, it has been noted that large field hysteresis losses usually involve in FOMT materials.[5] Because the field hysteresis losses are the costs in energy to make one cycle of the magnetic field, they must also be considered when calculating the RC of a magnetic refrigerant material being subjected to field cycling.[5] In the case of $Ni_{50}Mn_{50-x}Sn_x$ Heusler alloys, the hysteresis behavior is important and must be considered in evaluating RC for the case of the inverse MCE around $T_{M\text{-}A}$. In particular, for applied magnetic fields higher than a critical field (the field at which the metamagnetic transition occurs, meaning $\sim$3.5 T for $x = 13$ and $\sim$4 T for $x = 14$), magnetization process is not reversible and field hysteresis losses have been found to be significant. In this case, we have subtracted the average hysteretic losses from the RC values calculated without accounting for the hysteretic losses. After subtracting the large field hysteresis losses that accompany the metamagnetic first-order M-A transition, the RC values taken at 5 T for the $x = 13$ and 14 samples are found to decrease considerably from RC = 70 and 80 J/kg to 54 and 69 J/kg, respectively. These results suggest that for assessing the usefulness of a magnetocaloric material, one must take into account both ΔS_m and RC, particularly in the case of the metamagnetic transitions that can yield "giant" values of ΔS_m. Field hysteresis losses must also be considered and subtracted from the calculated RC for the case of FOMT materials.

In order to understand the difference in magnitude of $|\Delta S_{max}|$ values determined around the phase transitions in $Ni_{50}Mn_{50-x}Sn_x$ Heusler alloys, it is important to investigate their critical behaviors near these transitions. In the present

case, it is difficult to analyze the critical behavior of the martensitic second-order phase of $Ni_{50}Mn_{50-x}Sn_x$ ($x = 13$) ribbons, as martensitic FM and AFM states coexist and are close to the M-A transformation. For the austenitic phase, critical behaviors in the vicinity of T_C^A have been characterized by critical exponents of β, γ, and δ, which are associated with temperature dependences of the saturation magnetization $M_s(T)$, inverse initial susceptibility $\chi_0^{-1}(T)$, and critical isotherm M, respectively. Theoretically, the asymptotic relations in SOMTs are described by[18]

$$M_s(T) = M_0(-\varepsilon)^{\beta} \quad \text{for} \quad \varepsilon < 0, \tag{3}$$

$$\chi_0^{-1}(T) = (h_0/M_0)\varepsilon^{\gamma} \quad \text{for} \quad \varepsilon > 0, \tag{4}$$

$$M = DH^{1/\delta} \quad \text{for} \quad \varepsilon = 0, \tag{5}$$

where $\varepsilon = (T - T_C^A)/T_C^A$ is the reduced temperature, and M_0, h_0, and D are critical amplitudes. Additionally, in the critical region, the static-scaling hypothesis[18] predicts that the isothermal magnetization (M) is a universal function of ε and H

$$M(H, \varepsilon) = |\varepsilon|^{\beta} f_{\pm}(H/|\varepsilon|^{\beta+\gamma}), \tag{6}$$

where f_+ and f_- are regular functions for $T > T_C^A$ and $T < T_C^A$, respectively. This equation implies that, by plotting M/ε^{β} versus $H/\varepsilon^{\beta+\gamma}$, all data points with $T < T_C^A$ and $T > T_C^A$ are expected to fall into f_- and f_+ branches, respectively. The determination of the critical parameters (i.e., T_C^A, β, γ, and δ) is based on modified Arrott plots.[19] Detailed descriptions of the modified-Arrott method can be found elsewhere.[18,19] For $x = 13$, the critical values of $\beta = 0.385 \pm 0.035$ and $T_C^A = 303.4 \pm 0.6$ K from fitting $M_s(T)$ data to Eq. (3), and of $\gamma = 1.083 \pm 0.060$ and $T_C^A = 303.9 \pm 0.3$ K from fitting $\chi_0^{-1}(T)$ data to Eq. (4) were determined (Fig. 4(a)). Their averaged T_C^A value of 303.6 K is used for further discussion. With these critical parameters, the construction of M/ε^{β} versus $H/\varepsilon^{\beta+\gamma}$ plots reveals that the $M(H)$ data fall into two universal curves, one for temperatures below T_C^A (the f_- branch, associated with the FM phase) and the other for temperatures above T_C^A (the f_+ branch, associated with the PM phase, Fig. 4(b)). A similar analysis has been performed for the $x = 14$ sample. As shown in Figs. 4(c) and 4(d), this sample possesses $\beta = 0.496 \pm 0.015$, $\gamma = 1.024 \pm 0.059$, and $T_C^A = 304.5$ K (the average value). Using the Widom scaling relation of $\delta = 1 + \gamma/\beta$, we have obtained δ values of 3.82 and 3.01 for $x = 13$ and 14, respectively, which are close to those obtained from fitting isothermal magnetizations at temperatures $T \approx T_C^A$ to Eq. (5). These results prove the reliability of the T_C^A, β, and γ values obtained in our work.

In comparison with the results obtained from the standard models, including mean-field theory (MFT, $\beta = 0.5$, $\gamma = 1.0$, and $\delta = 3.0$), the 3D Heisenberg model ($\beta = 0.365$, $\gamma = 1.336$, and $\delta = 4.80$), and the 3D Ising model ($\beta = 0.325$, $\gamma = 1.241$, and $\delta = 4.82$),[18] we find that the γ values obtained from the present ribbon samples ($\gamma = 1.083$ and 1.024 for $x = 13$ and 14, respectively) are very close to that of MFT ($\gamma = 1.0$). This suggests that the $x = 13$ and 14 ribbons exhibit a similar PM characteristic at temperatures $T > T_C^A$. This hypothesis is supported by the fact that the data of $M(H)$ as $T > T_C^A$ fall completely into the f_+ branch (see Figs. 4(b) and 4(d)). However, the situation becomes different when the critical behaviors of the austenitic FM phase are examined. While the β value of the $x = 13$ sample is close to that expected for the 3D Heisenberg model, the β value of the $x = 14$ sample is close to that expected for MFT. This points to the existence of a short-range FM order in the $x = 13$ sample, but a long-range FM order in the $x = 14$ sample for $T < T_C^A$. The occurrence of the short-range FM order in the $x = 13$ sample is reasonable, due to the co-existence of FM/AFM interactions associated with the martensitic phase

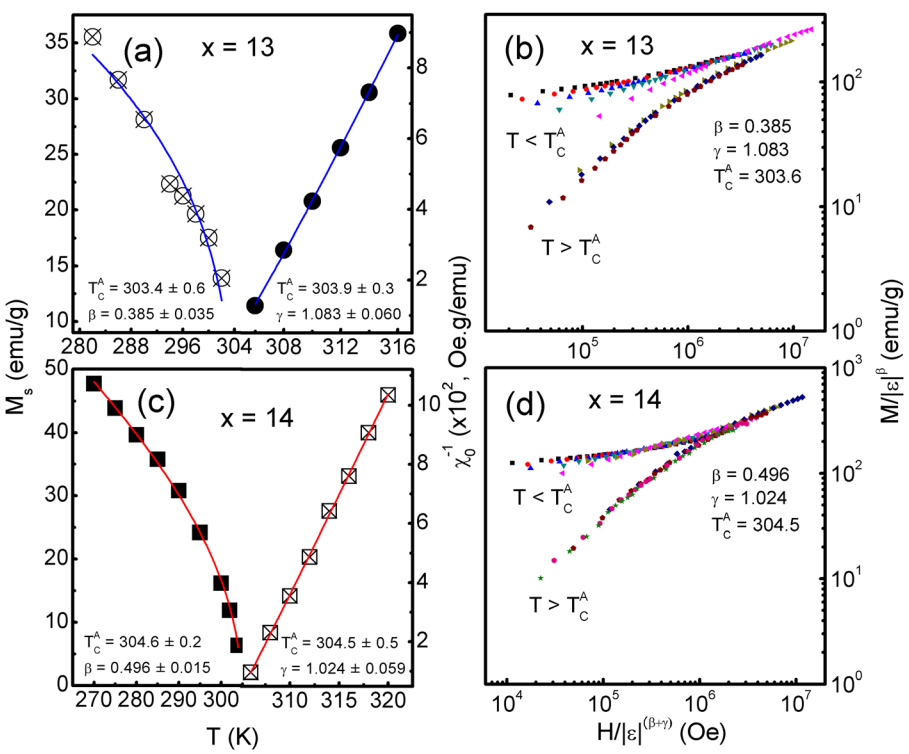

FIG. 4. $M_s(T)$ and $\chi_0^{-1}(T)$ data fitted to the critical relations and static-scaling performances for $Ni_{50}Mn_{50-x}Sn_x$ with (a), (b) $x = 13$ and (c), (d) $x = 14$.

and the M-A transformation.[8,16] This is reflected by small deviation of the $M_s(T)$ data around 294 K from the fitting curve (Fig. 4(a)) and the scattering of some $M(H)$ point data at temperatures $T < T_C^A$ from the f_- branch (Fig. 4(b)). For the $x = 14$ sample, the austenitic phase is dominant over the martensitic one, so the occurrence of the long-range FM order is expected. This is supported by the observation that the experimental data of $M_s(T)$, $\chi_0^{-1}(T)$, and $M(H)$ around T_C^A are well described by the asymptotic relations (Figs. 4(c) and 4(d)). Notably, the transformation of short-to-long range FM orders as the x value in $Ni_{50}Mn_{50-x}Sn_x$ changed from 13 to 14, respectively, reduces the ΔS_m slightly but enhances RC significantly at a given field and reduces the impact of field hysteresis losses around $T_{M\text{-}A}$.

In summary, we have systematically studied the conventional and inverse magnetocaloric effects and critical behaviors in melt-spun $Ni_{50}Mn_{50-x}Sn_x$ ($x = 13$ and 14) ribbons. We show that although the magnetic entropy change associated with the SOMT is about five times smaller than that associated with FOMT, the refrigerant capacity is larger for the former case. The hysteresis losses are large and significantly reduce RC in the case of the FOMT. Our study confirms that large ΔS_m should not be the sole factor in assessing the usefulness of a magnetocaloric material, and magnetic hysteresis losses must be taken into account for RC in the case of FOMT materials. The Sn addition has been found to transform the $Ni_{50}Mn_{50-x}Sn_x$ system, in the austenitic ferromagnetic phase, from the short-range ($x = 13$) to long-range ($x = 14$) ferromagnetic order.

This research was supported by the Converging Research Center Program funded by the Ministry of Education, Science and Technology (2012K001431) and partly supported by the National Foundation for Science and Technology Development (NAFOSTED) of Vietnam under Grant No. 103.02-2011.23. M.H.P. also acknowledges the support from the Florida Cluster for Advanced Smart Sensor Technologies (FCASST).

[1]A. M. Tishin and Y. I. Spichkin, *The Magnetocaloric Effect and its Applications* (Institute of Physics Publishing, Bristol and Philadelphia, 2003).
[2]V. K. Pecharsky, K. A. Gschneidner, and A. O. Tsokol, Rep. Prog. Phys. **68**, 1479 (2005).
[3]E. Bruck, J. Phys. D: Appl. Phys. **38**, R381 (2005).
[4]M. H. Phan and S. C. Yu, J. Magn. Magn. Mater. **308**, 325 (2007).
[5]V. Provenzano, A. J. Shapiro, and R. D. Shull, Nature **429**, 853 (2004).
[6]R. Caballero-Flores, V. Franco, A. Conde, K. E. Knipling, and M. A. Willard, Appl. Phys. Lett. **98**, 102505 (2011).
[7]A. Chaturvedi, S. Stefanoski, M. H. Phan, G. S. Nolas, and H. Srikanth, Appl. Phys. Lett. **99**, 162513 (2011).
[8]T. Krenke, E. Duman, M. Acet, E. F. Wassermann, X. Moya, L. Mañosa, and A. Planes, Nature Mater. **4**, 450 (2005).
[9]T. Krenke, M. Acet, E. F. Wassermann, X. Moya, L. Mañosa, and A. Planes, Phys. Rev. B **72**, 014412 (2005).
[10]J. Du, Q. Zheng, W. J. Ren, X. G. Liu, and Z. D. Zhang, J. Phys. D: Appl. Phys. **40**, 5523 (2007).
[11]A. K. Nayak, K. G. Suresh, and A. K. Nigam, J. Phys. D: Appl. Phys. **42**, 035009 (2009)
[12]V. D. Buchelnikov and V. V. Sokolovskiy, Phys. Met. Metallogr. **112**, 633 (2011).
[13]P. J. Shamberger and F. S. Ohuchi, Phys. Rev. B **79**, 144407 (2009).
[14]V. V. Khovaylo, K. P. Skokov, O. Gutfleisch, H. Miki, T. Takagi, T. Kanomata, V. V. Koledov, V. G. Shavrov, G. Wang, E. Palacios, J. Bartolomé, and R. Burriel, Phys. Rev. B **81**, 214406 (2010).
[15]V. Basso, C. P. Sasso, K. P. Skokov, O. Gutfleisch, and V. V. Khovaylo, Phys. Rev. B **85**, 014430 (2012).
[16]M. Khan, I. Dubenko, S. Stadler, and N. Ali, J. Appl. Phys. **102**, 113914 (2007).
[17]V. K. Pecharsky, and K. A. Gschneidner, Jr, J. Appl. Phys. **90**, 4614 (2001).
[18]H. E. Stanley, *Introduction to Phase Transitions and Critical Phenomena* (Oxford University Press, London, 1971).
[19]A. Arrott and J. E. Noakes, Phys. Rev. Lett. **19**, 786 (1967).